



◀ Data Products & Services

Sea Ice Concentrations from Nimbus-7 SMMR and DMSP SSM/I Passive Microwave Data

[Documentation](#) [Register for Data](#)

The NASA Goddard Space Flight Center (GSFC) sea ice concentration data set in the polar stereographic projection is derived from the Scanning Multichannel Microwave Radiometer (SMMR) and Special Sensor Microwave/Imager (SSM/I) data using the NASA Team algorithm. It is designed to provide a consistent time series of sea ice concentrations (the fraction of ocean area covered by sea ice) spanning the coverage of several passive microwave instruments. To aid in this goal, sea ice algorithm coefficients are changed to reduce differences in sea ice extent and area as estimated using the SMMR and SSM/I sensors.

The data set currently includes daily and monthly averaged sea ice concentrations derived from Nimbus-7 SMMR and DMSP-F8, -F11 and -F13 SSM/I daily brightness temperatures at a grid cell size of 25 x 25 km. The data set begins October 1978 and continues through December 2004. Data are available via FTP. Data files are stored as flat binary data with one byte per pixel. For each data file, a corresponding graphics file in GIF format is provided. These sea ice concentrations are generated by the Oceans and Ice Branch, Laboratory for Hydrospheric Processes at NASA GSFC, using SMMR brightness temperatures that were processed at NASA GSFC and SSM/I brightness temperatures that were



Data Contributors

- CAVALIERI, DONALD
- PARKINSON, CLAIRE L.
- GLOERSEN, PER
- ZWALLY, H. JAY

Parameters

- ICE EXTENT
- SEA ICE CONCENTRATION

Instruments

- SMMR : SCANNING MULTICHANNEL MICROWAVE RADIOMETER
- SSM/I : SPECIAL SENSOR MICROWAVE/IMAGER

processed at the National Snow and Ice Data Center (NSIDC). Both of these data sets are archived at NSIDC.

Data Citation

The following example shows how to cite the use of this data set in a publication. List the principal investigators, year of data set release, data set title, dates of data you used, publishers (NSIDC), and digital media.

Cavalieri, D., C. Parkinson, P. Gloerson, and H.J. Zwally. 1997, updated 2005. *Sea ice concentrations from Nimbus-7 SMMR and DMSP SSM/I passive microwave data*, June to September 2001. Boulder, CO, USA: National Snow and Ice Data Center. Digital media.

See Also

- [Sea Ice Products at NSIDC](#)
- [Sea Ice Remote Sensing at NASA Goddard Space Flight Center](#)
- [Contact User Services](#)



The National Snow and Ice Data Center ([NSIDC](#))

Supporting Cryospheric Research Since 1976

[CIRES](#), 449 UCB University of Colorado Boulder, CO 80309-0449

[NSIDC privacy policy](#) | [Use/Copyright Info](#)



Sea Ice Concentrations from Nimbus-7 SMMR and DMSP SSM/I Passive Microwave Data

Summary

The NASA Goddard Space Flight Center (GSFC) sea ice concentration data set in the polar stereographic projection is derived from the Scanning Multichannel Microwave Radiometer (SMMR) and Special Sensor Microwave/Imager (SSM/I) data using the NASA Team algorithm. It is designed to provide a consistent time series of sea ice concentrations (the fraction of ocean area covered by sea ice) spanning the coverage of several passive microwave instruments. To aid in this goal, sea ice algorithm coefficients are changed to reduce differences in sea ice extent and area as estimated using the SMMR and SSM/I sensors.

The data set currently includes daily and monthly averaged sea ice concentrations derived from Nimbus-7 SMMR and DMSP-F8, -F11 and -F13 SSM/I daily brightness temperatures at a grid cell size of 25 x 25 km. The data set begins October 1978 and continues through December 2004. Data are available via FTP. Data files are stored as flat binary data with one byte per pixel. For each data file, a corresponding graphics file in GIF format is provided. These sea ice concentrations are generated by the Oceans and Ice Branch, Laboratory for Hydrospheric Processes at NASA GSFC, using SMMR brightness temperatures that were processed at NASA GSFC and SSM/I brightness temperatures that were processed at the National Snow and Ice Data Center (NSIDC). Both of these data sets are archived at NSIDC.

This document is limited to description of the sea ice concentration product and product format, and includes only basic information on the sensors and raw data. Links and references are provided to give users background information on the sensors and data sets used to generate the sea ice product.

Citing These Data

To broaden awareness of our services, NSIDC requests that you acknowledge the use of data sets distributed by NSIDC. Please refer to the citation in this documentation for the suggested form, or [contact NSIDC User Services](#) for further information. We also request that you send us one reprint of any publication that cites the use of data received from our Center. This helps us to determine the level of use of the data we distribute. Thank you.

The following example shows how to cite the use of this data set in a publication. List the principal investigators, year of data set release, data set title, dates of data you used, publishers (NSIDC), and digital media.

Cavalieri, D., C. Parkinson, P. Gloerson, and H.J. Zwally. 1996, updated 2005. *Sea ice concentrations from Nimbus-7 SMMR and DMSP SSM/I passive microwave data*, June to September 2001. Boulder, CO, USA: National Snow and Ice Data Center. Digital media.

Overview Table

Category	Description
Data format	Each file consists of a 300-byte header followed by 1-byte flat binary arrays: 304 columns x 448 rows (North) and 316 columns x 332 rows (South). A corresponding GIF image is also provided with each file.
Spatial coverage and resolution	North and south polar regions at 25 km resolution
Temporal coverage and resolution	Data extend from 26 October 1978 through 31 December 2004. SMMR data were collected every other day, and SSM/I data were collected daily. This data set provides daily and monthly averages throughout the time series.
Tools for accessing data	Software for reading and displaying sea ice concentration files is provided on the FTP site. Included are tools to ingest and read sea ice concentration data, determine geolocation of data, display, extract and export the data, as well as masking tools that limit the influence of non-sea ice brightness temperatures (T_{BS}).
Data range	Data are stored as 1-byte integers representing sea ice concentration values. The sea ice concentration data values are packed into byte format by multiplying the original sea ice concentration floating-point values (ranging from 0.0 to 1.0) by a scaling factor of 250.
Grid type and size	North: 304 columns x 448 rows South: 316 columns x 332 rows
File naming convention	yyyymmdd.hss
File size	Northern files: 134 KB Southern files: 103 KB
Parameter(s)	Sea ice concentration
Procedures for obtaining data	Data are available via FTP for the entire time series (through 2004). Please contact NSIDC User Services to place an order.

Table of Contents

- [1. Contacts and Acknowledgments](#)
- [2. Detailed Data Description](#)
- [3. Data Access and Tools](#)

- [4. Data Acquisition and Processing](#)
- [5. References and Related Publications](#)
- [6. Document Information](#)

1. Contacts and Acknowledgments

Investigator(s) Name and Title

Donald J. Cavalieri, Claire L. Parkinson, Per Gloersen, and H. Jay Zwally

NASA Goddard Space Flight Center (GSFC)

Greenbelt, MD, USA

Technical Contact

NSIDC User Services

National Snow and Ice Data Center

CIRES, 449 UCB

University of Colorado

Boulder, CO 80309-0449 USA

phone: +1 303.492.6199

fax: +1 303.492.2468

form: [Contact NSIDC User Services](#)

e-mail: nsidc@nsidc.org

2. Detailed Data Description

This document provides a description of a sea ice concentration time series data set generated from T_{BS} derived from SMMR and SSM/I radiances. The data set includes gridded daily and monthly averaged sea ice concentrations (every other day for SMMR data) for both the north and south polar regions from 26 October 1978 through 31 December 2004. See the [DMSP SSM/I Daily and Monthly Polar Gridded Sea Ice Concentrations](#) for more recent sea ice concentration data.

No data coverage is available for regions poleward of 81° latitude for SMMR and 87° for SSM/I due to the inclination of the orbits. SMMR data were acquired every other day, while SSM/I data are acquired daily.

The goal in the creation of the data set is to produce a long term, consistent set in which sea ice extent and area differences between the sensors are reduced and could serve as a baseline for future measurements. This document describes the basic characteristics of the SMMR and SSM/I platforms and summarizes the problems encountered when deriving sea ice concentrations from T_{BS} measured by sensors with different frequencies, different footprint sizes, different visit times, and different calibrations. A major obstacle to resolving these differences is the lack of sufficient overlapping data from sequential sensors. The techniques employed to reduce the effects of these problems are presented.

Basic limitations arise from the sensor resolution, temporal coverage, and algorithm assumptions and characteristics. You should review the information provided on fields of view, temporal sampling, and algorithm characteristics.

Particular care is needed to interpret the sea ice concentrations during summer when melt is present, and in regions where new sea ice makes up a substantial part of the sea ice cover. As noted, some residual errors remain due to weather effects and mixing of ocean and land area within the sensor field of view and due to sensor differences.

The NASA Team algorithm is not designed to provide ice concentration for fresh-water ice (e.g., lake and river ice). The filtering used to remove land-to-ocean spill over may affect the area of some open water features within the ice pack near coasts (e.g., coastal polynyas). Users concerned with detailed analyses of near-coastal conditions are encouraged to compare these data with the [DMSP SSM/I Daily and Monthly Polar Gridded Sea Ice Concentrations](#).

You should also be aware that the ice concentration maps were derived from algorithms that were "tuned" to minimize the differences in ice extent and ice covered area during the overlap periods (e.g. between SMMR and SSM/I-F8 and between SSMI-F8 and-SSM/I F11). This does not necessarily mean that the ice concentrations themselves are well matched. See the [Data Verification by Data Center](#) section of this document for a summary of ice extent and ice covered area differences during the overlap periods.

Applications for these sea ice concentration data include:

- Monitoring the distribution, extent, and area of the Arctic and Antarctic sea ice cover.
- Mapping the variability in the fraction of open water/thin ice within the ice pack.
- Identifying and monitoring persistent open-water areas (polynyas) (see the related note in Section 6).
- Analyses of regional and global trends in sea ice cover.
- Estimating new sea ice formation and brine production.
- Validation of sea ice models and climate models.
- Analysis of sea ice/ocean and sea ice/atmosphere interactions.

Format

Data files are stored in original GSFC format: flat binary data with one byte per pixel. For each data file, a corresponding graphics file in GIF format is provided. The file format used for this SMMR and SSM/I sea ice concentration data set consists of a 300-byte descriptive header followed by a two-dimensional array of 1-byte values containing the data.

The file header is composed of four components: a 21-element array of 6-byte character strings containing information such as polar stereographic grid characteristics, a 24-byte character string containing the file name, an 80-character string containing an optional image title, and a 70-byte character string containing ancillary information such as data origin, dataset creation date, etc. For compatibility with ANSI C, IDL, and other languages, the aforementioned character strings are terminated with a NULL byte.

The file header can be accessed in a variety of different ways. It can be treated as a simple sequence of bytes containing ASCII character strings (unsigned char type in ANSI C) or as a complex data structure of BYTE arrays in IDL.

Header Byte Descriptions

Bytes	Description
1-6	Missing data integer value
7-12	Number of columns in polar stereographic grid
13-18	Number of rows in polar stereographic grid
19-24	Scale factor (10^6)
25-30	Latitude enclosed by polar stereographic grid
31-36	Greenwich orientation of polar stereographic grid
37-42	Radius of Earth
43-48	J-coordinate of the grid intersection at the pole
49-54	I-coordinate of the grid intersection at the pole
55-60	5-character instrument descriptor (SMMR, SSM/I)
61-66	Two descriptors of two characters each that describe the data; For example, 07 cn = Nimbus-7 SMMR ice concentration
67-72	Starting Julian day of grid data
73-78	Starting hour of grid data (if available)
79-84	Starting minute of grid data (if available)
85-90	Ending Julian day of grid data
91-96	Ending hour of grid data (if available)
97-102	Ending minute of grid data (if available)
103-108	Year of grid data
109-114	Julian day of grid data
115-120	Three-digit channel descriptor (000 for ice concentrations)
121-126	Integer scaling value with which the floating point
127-150	24-character file name
151-230	80-character image title
231-300	70-character data information (creation date, data source, etc.)

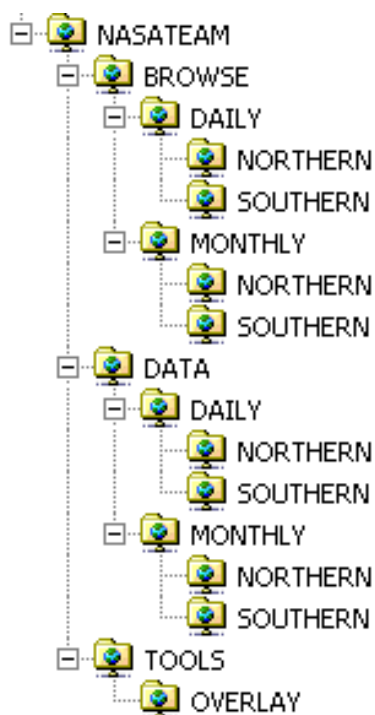
The GSFC-formatted data can be read with image processing software by specifying a 300-byte header, with an image size of 304 columns x 448 rows for Arctic data and 316 columns x 332 rows for Antarctic data. In a

high-level programming language or IDL, declare a 300-byte array for the header and a 304 x 448 (Arctic) array for the image. Read the 300-byte array first, then read the image array. See examples supplied with the data for more details.

Sea ice concentration values are packed into byte format by multiplying the original sea ice concentration floating-point values (ranging from 0.0 to 1.0) by a scaling factor of 250. Thus a sea ice concentration value of 0% (0.0) maps to a byte value of 0 and a sea ice concentration value of 100% (1.0) maps to a value of 250. To revert back to the original range of 0.0 to 1.0, divide the scaled sea ice concentrations by 250.0.

File and Directory Structure

The directory structure on the [FTP](#) site is as follows:



File Naming Convention

Data files are zipped together on the FTP site in "gzipped tar" format by year. The "Daily" files are named:

yyyyh.tar.gz

Where:

yyyy = four-digit year

h = hemisphere ("n" or "s")

The individual "daily" files are named as follows:

yyyymmdd.hss

Where:

yyyy = four-digit year

mm = two-digit month

dd = two-digit day

h = hemisphere ("n" or "s")

ss = two-digit sensor indicator (07, 08, 11, or 13 for Nimbus-7 SMMR or DMSP-F8, -F11 and -F13 SSM/I)

The file naming convention for the "monthly" files is similar:

yyyh_MONTHLY.tar.gz (includes _MONTHLY)

yyyymm.hss (no two-digit day)

File Size

Northern files: 134 KB

Southern files: 103 KB

Spatial Coverage

Data set coverage is of the polar regions and is defined by the spatial coverage map described below. SSM/I instrument coverage is global except for circular sectors centered over the pole, 280 km in radius, located poleward of 87°, which are never measured due to orbit inclination. The measurement footprint size (effective field of view) is as follows:

SSM/I

Channel	Footprint size
19.3 GHz	70x45 km
22.2 GHz	60x40 km
37.0 GHz	38x30 km

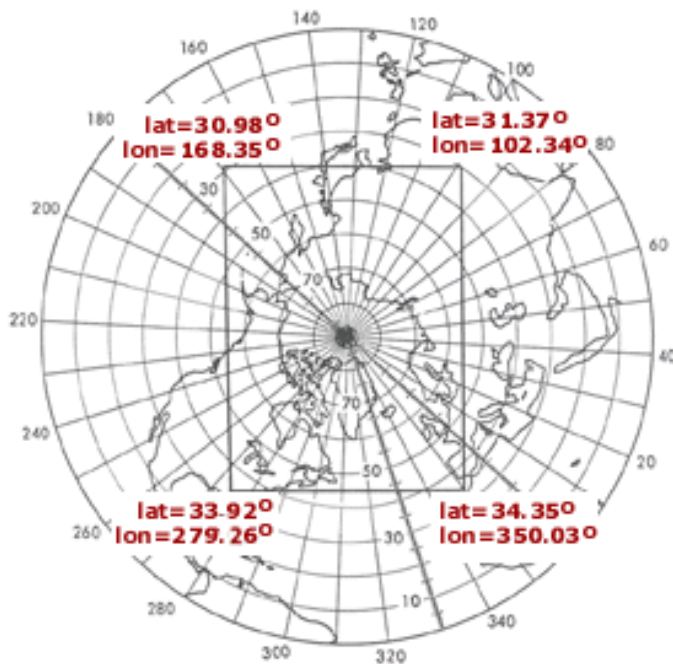
SMMR instrument coverage is global except for circular sectors centered over the pole, approximately 611 km in radius, located poleward of 84.7°. The 50° scan pattern mapped out a swath width of 780 km at the Earth's surface. The spatial resolutions at the various frequencies ranged from approximately 27 km at 37 GHz to 148 km at 6.6 GHz. The measurement footprint size is as follows:

SMMR

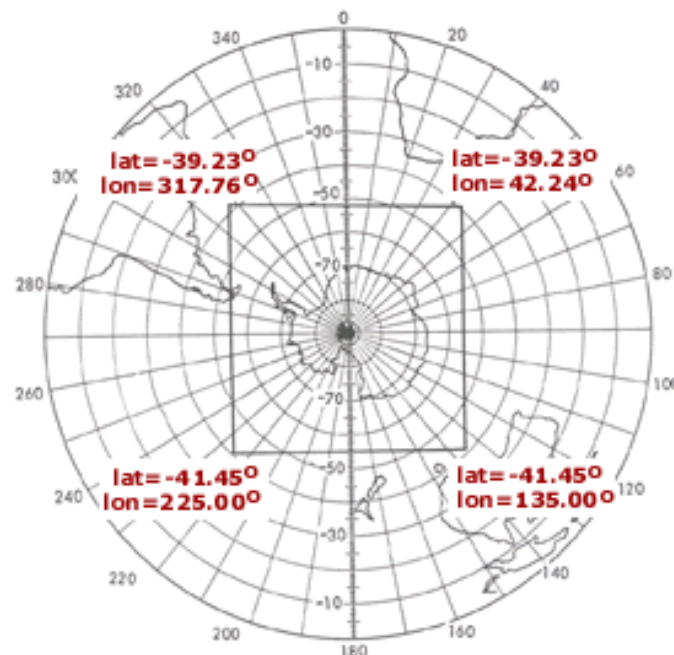
Channel	Footprint size
6.6 GHz	148x95 km
10.7 GHz	91x59 km
18.0 GHz	55x41 km

21.0 GHz	46x30 km
37.0 GHz	27x18 km

Spatial Coverage Map



Northern Hemisphere



Southern Hemisphere

Spatial Resolution

The footprint sizes of SMMR and SSM/I observations are given in the [Spatial Coverage](#) section. These footprints are mapped to a 25 km grid spacing.

Projection

T_B grids are in a polar stereographic projection, which specifies a projection plane (i.e., the grid) tangent to the earth at 70° . The planar grid is designed so that the grid cells at 70° latitude are 6.25 km x 6.25 km. For more information on this topic please refer to [Pearson \(1990\)](#) and [Snyder \(1987\)](#).

The polar stereographic projection often assumes that the plane (grid) is tangent to the Earth at the pole. Thus, there is a one-to-one mapping between the Earth's surface and grid (with no distortion) at the pole. Distortion in the grid increases as the latitude decreases because more of the Earth's surface falls into any given grid cell, which can be quite significant at the edge of the northern polar grid where distortion reaches 31%. The southern polar grid has a maximum distortion of 22%. To minimize the distortion, the projection is true at 70° rather than the poles. This increases the distortion at the poles by three percent and decreases the distortion at the grid boundaries by the same amount. The latitude of 70° was selected so that little or no

distortion would occur in the marginal ice zone. Another result of this assumption is that fewer grid cells will be required as the Earth's surface is more accurately represented.

The polar stereographic formulae for converting between latitude/longitude and X-Y grid coordinates are taken from [Snyder \(1982\)](#). This projection assumes a Hughes ellipsoid with a radius of 3443.992 nautical mi or 6378.273 km and an eccentricity (e) of 0.081816153 (or $e^2 = 0.006693883$).

Grid Description

Hemisphere	Grid size	Nominal grid cell size
North	304 columns x 448 rows	25 km
South	316 columns x 332 rows	25 km

The origin of each x, y grid is the pole. The grids' approximate outer boundaries are defined in the following table. Corner points are listed; apply values to the polar grids reading clockwise from upper left. Interim rows define boundary midpoints.

	X(km)	Y(km)	Latitude (deg)	Longitude (deg)	
North Polar:	-3850	5850	30.98	168.35	corner
	0	5850	39.43	135.00	midpoint
	3750	5850	31.37	102.34	corner
	3750	0	56.35	45.00	midpoint
	3750	-5350	34.35	350.03	corner
	0	-5350	43.28	315.00	midpoint
	-3850	-5350	33.92	279.26	corner
	-3850	0	55.50	225.00	midpoint

	X(km)	Y(km)	Latitude (deg)	Longitude (deg)	
South Polar	-3950	4350	-39.23	317.76	corner
	0	4350	-51.32	0.00	midpoint
	3950	4350	-39.23	42.24	corner
	3950	0	-54.66	90.00	midpoint
	3950	-3950	-41.45	135.00	corner
	0	-3950	-54.66	180.00	midpoint
	-3950	-3950	-41.45	225.00	corner
	-3950	0	-54.66	270.00	midpoint

Temporal Coverage

This data set begins October 1978 and continues through December 2004.

Temporal Resolution

SMMR data were collected every other day. (The scanner operated only on alternate days, due to spacecraft power limitations). Typically, there are at least 14 days of coverage per month, although major data gaps occur in August of 1982 (4, 8, and 16 August 1982) and 1984 (13 through 23 August 1984) for both polar regions.

SSM/I data are collected daily. Ice concentrations are provided for each day of data and as monthly means. The monthly mean files are generated by averaging all the available daily files for each individual month, excluding pixels of missing data (see [Processing Monthly Means section of this document for more information](#)). A major data gap in the SSM/I data occurs from 3 December 1987 to 13 January 1988.

Parameter or Variable

Parameter Description

Sea ice concentration represents an areal coverage of sea ice. For a given grid cell, the parameter provides an estimate of the amount of sea ice covering that cell, with the remainder of the area consisting of open ocean. Land areas are coded with a land mask value.

Unit of Measurement

Percentage of sea ice

Parameter Source

Nimbus-7 SMMR and DMSP-F8, -F11 and -F13 SSM/I.

Parameter Range

Data are stored as 1-byte integers representing sea ice concentration values. The sea ice concentration data values are packed into byte format by multiplying the original sea ice concentration floating-point values (ranging from 0.0 to 1.0) by a scaling factor of 250. Thus a sea ice concentration value of 0% (0.0) maps to a byte value of 0 and a sea ice concentration value of 100% (1.0) maps to a value of 250. To revert back to the original range of 0.0 to 1.0, divide the scaled ice concentrations by 250.0.

The superimposed land mask is assigned a byte value of 254, coastlines are assigned a value of 253, the circular mask used in the Arctic to cover the irregularly-shaped data gap around the pole (caused by the orbit inclination and instrument swath) is 251, and all other missing data are assigned the value 255.

Error Sources

Before March 2002, the latitude and longitude files accompanying this product were in error for both hemispheres. (An online [error notice](#) details the problem.) Corrected versions of these files are available via

[FTP](#).

NSIDC discovered in December 1999 that the original "showice.pro" routine contained a coding error related to reading files with .N13 and .S13 extensions. The coding error has been fixed and a corrected version of this routine is available via [FTP](#).

The original version of the Matlab routine, showice.m, contained a coding error. A corrected 'showice.m' is available via [FTP](#).

Pixel area files (pixlarea.n and pixlarea.s) were also found to be in error, and corrected versions are available via [FTP](#).

Data Validation by Source

The performance of the NASA Team Algorithm was assessed in numerous studies (e.g., [Cavalieri et al. 1992](#)). These results apply to the combined SMMR-SSM/I time series described here. Improvements in this data set that differ from these previous studies include the minimization of coastal and open-ocean influences that tend to yield inaccurate sea ice concentrations. Visual data checking was used to assess the performance of these modifications.

Confidence Level/Accuracy Judgment

Estimates of the accuracy of the NASA Team Algorithm vary depending on sea ice conditions, methods, and locations used in individual studies. [Cavalieri et al. \(1992\)](#) summarizes several of these studies. In general, accuracy of total sea ice concentration is approximately 5% (e.g., within 5% of the actual sea ice concentration) in winter, and approximately 15% in the Arctic during summer when melt ponds are present on the sea ice. Accuracy tends to be best within the consolidated ice pack when the sea ice is relatively thick (greater than 20 cm) and ice concentration is high. Accuracy decreases as the proportion of thin ice increases. Accuracy is better in the Antarctic, but standard deviations are larger ([Cavalieri et al. 1992](#)). See [Cavalieri et al. \(1992\)](#), [Steffen et al. \(1992\)](#), and others in the attached reference list for an overview of the algorithm performance.

Data Verification by Data Center

NSIDC staff visually checked the entire set of data files and selected graphics files. This included checks for proper file structure, comparisons to existing SMMR- and SSM/I-derived sea ice concentration grids, masks, and information files and examination of data quality.

Some weather-related effects and land contamination are still present, but are reduced compared to the [DMSP SSM/I Daily and Monthly Polar Gridded Sea Ice Concentrations](#). The amount and spatial distribution of those remaining weather effects varies with season. Also, occasional bad scan lines still appear in the data. Based on NSIDC analyses (see NSIDC's [Special Publication 5](#) for summaries of differences among the SSM/I sensors), some sensor-to-sensor differences are likely to remain in these data, particularly for marginal ice zones. Further evaluation by NSIDC is planned.

During May 1986, residual weather effects and processing errors result in large bands of very low ice

concentrations over the open ocean in the Weddell, Bellingshausen, and Amundsen seas in the Southern Hemisphere. Although the magnitude of these false ice concentrations is less than one percent, users should be aware that such errors do occur for many days within that month.

In creating the time-series data set, differences in ice extent and ice covered area during the overlap periods (e.g. between SMMR and DMSP-F8, DMSP-F8 and -F11, and between DMSP-F11 and -F13) were minimized by tuning the sea ice algorithms. Wavelet analysis of the time-series of ice extent and ice covered area show no significant offsets between the different satellites. The following table summarizes the comparison between the ice extent and ice covered areas during the overlap periods.

Mean differences and linear regression results of ice extent and ice covered area for the overlap periods. Mean differences are computed for SMMR minus SSM/I F8, SSM/I F8 minus SSM/I F11, and SSM/I F13 minus SSM/I F11. Regression coefficients are computed using $x = \text{SMMR}$, $y = \text{SSM/I F8}$, $x = \text{SSM/I F8}$, $y = \text{SSM/I F11}$, and $x = \text{SSM/I F11}$, $y = \text{SSM/I F13}$, where $y = a_0 + a_1 \cdot x$.

North

	Mean difference (x 10 ⁶ km ²)	Standard deviation (x 10 ⁶ km ²)	A ₀ (x 10 ⁶ km ²)	A ₁	Correlation coefficient	% difference
SMMR/SSMI-F8						
ice area	0.073	0.054	0.214	0.947	0.999	1.34%
ice extent	0.055	0.096	0.412	0.941	0.998	0.70%
SMMR/SSMI-F11						
ice area	-0.019	0.036	0.955	0.914	0.996	0.18%
ice extent	0.002	0.058	0.351	0.972	0.983	0.01%
SMMR/SSMI-F13						
ice area	-0.0112	0.0296	0.0079	0.997	0.999	0.18%
ice extent	-0.0004	0.0457	0.0199	0.997	0.999	-0.01%

South

	Mean difference (x 10 ⁶ km ²)	Standard deviation (x 10 ⁶ km ²)	A ₀ (x 10 ⁶ km ²)	A ₁	Correlation coefficient	% difference
SMMR/SSMI-F8						
ice area	0.018	0.072	0.225	0.982	0.992	0.15%
ice extent	0.005	0.058	-0.198	1.011	0.998	0.0%
SMMR/SSMI-F11						

ice area	-0.038	0.092	0.630	0.924	0.996	0.49%
ice extent	0.012	0.067	0.289	0.974	0.998	0.08%
SMMR/SSMI-F13						
ice area	0.0311	0.0344	-0.0474	1.007	0.999	0.26%
ice extent	0.0126	0.0402	-0.0186	1.002	0.999	0.08%

While this analysis shows no significant differences between the overall summaries of ice extent and ice-covered area, significant regional difference in ice concentration may still be present.

3. Data Access and Tools

Data Access

Data are [available via](#) FTP. Please contact [NSIDC User Services](#) to place an order.

Software and Tools

Software for reading and displaying the files is provided on the [FTP](#) site. The GSFC file structure and sample codes for reading the data are also provided. Software includes IDL and Matlab routines to ingest and read sea ice concentration data. The IDL procedure was tested on several UNIX workstations. The Matlab procedure has been tested on a SG-IRIX machine, and on a PC Pentium machine under Windows for Workgroups 3.11. Cross-platform capabilities of Matlab should also permit operation on Macintosh, but this has not been tested.

Tools

GSFC tools for the time series data set include grids of North Polar and South Polar pixel areas; X/Y-to-Latitude and -Longitude conversion matrices; IDL & Matlab software to ingest and read ice concentration data; and Mac and DOS GIF viewers. GSFC software includes:

showice.m - A Matlab program that will display an image of the sea ice concentration grids in either of two color scales. The version of this program that was originally distributed on CD contained a coding error. A corrected 'showice.m' is available via [FTP](#).

showice.pro - An IDL program, available by [FTP](#), that will display images of the sea ice concentration grids or of the GIF images themselves (automatically). Note that this program does not support the latitude and longitude files listed below. Also note that IDL Version 5.4 and higher does not support reading or writing GIF images. Users using IDL Version 5.4 and higher will therefore not be able to view the GIF images using the program "showice.pro." An alternative format for IDL 5.4 and higher is Portable Network Graphics (PNG).

ombra.exe - A DOS program for viewing GIF images. (Also works in Windows 3.11 by double-clicking on

the file entry in File Manager.) This freeware is provided through the courtesy of Rick Ostidich, whose e-mail address is ostidich@enet.it (URL: <http://www.enet.it/hpg/ew>).

JPEGview - A Mac program for viewing GIF images.

readfile.pro - An IDL program for ingesting ice concentration data files. Pieces may be useful as building blocks in other IDL programs users may want to develop.

pixlarea.n (pixlarea.s) - A matrix of grid cell areas for the Arctic (Antarctic) polar stereographic projection used here. This file can be used as a lookup table to determine the area in square meters of any grid cell. The file contains the standard 300-byte header, then an unformatted (and no FORTRAN record descriptor words) 2-dimensional, 4-byte (long) integer array of 448 rows x 304 columns (stored by rows in column order), for the Northern Hemisphere and 332 rows x 316 columns for the Southern Hemisphere grid. Pixel area files were updated in March 2002.

latitude.n (latitude.s) - This file contains a two-dimensional array of latitudes corresponding to the Arctic (Antarctic), X/Y polar stereographic grid values. This file can be used as a lookup table to determine the latitude value of any grid cell. The file consists of a standard 300-byte header followed by a 2-dimensional, 4-byte (long) integer array of 448 rows x 304 columns for the Northern Hemisphere, stored by rows in column order. Note that the values must be divided by one million to obtain degrees and decimal fractions. The latitudes range from 0.0 to 90.0 (-0.0 to -90.0) degrees.

longitude.n (longitude.s) - This tool is the same as for the latitudes above but the longitudes range from 0.0 degrees to 360.0 degrees EAST longitude.

Masks

landmask.n (landmask.s) - A recently revised land mask for the Arctic polar stereographic grid, taking into account more fully antenna spill over effects. This land mask is described in NASA Technical Memorandum 104625. This file has a standard 300-byte header and is a 2-dimensional byte array of 448 rows x 304 columns (332 rows x 316 columns), stored by rows in column order. Ocean areas are assigned byte values of 0. Land areas are assigned byte values of 1. Coastlines are assigned byte values of 2. Note that the ice concentration grids already have this landmask applied -- with different byte values.

gsfc_25n.hdf - North 25 km land mask

gsfc_25s.hdf - South 25 km land mask

sectmask.n (sectmask.s) The Arctic (Antarctic) region mask for the polar stereographic grid used here.

This region mask is described further in: "Arctic and Antarctic Sea Ice, 1978-1987 Satellite Passive Microwave Observations and Analysis," NASA SP-511.

The file contains a standard 300-byte header, followed by a 2-dimensional byte array of 448 rows x 304 columns (332 x 316) stored by rows in column order. Regions are assigned different pixel values as follows:

Arctic

Pixel value	Region
1	Non-regional ocean
2	Sea of Okhotsk and Japan
3	Bering Sea
4	Hudson Bay
5	Baffin Bay/Davis Strait/Labrador Sea
6	Greenland Sea
7	Kara and Barents Seas
8	Arctic Ocean
9	Canadian Archipelago
10	Gulf of St. Lawrence
11	Land
12	Coast
0	Lakes, extended coast

Antarctic

Pixel value	Region
2	Weddell Sea
3	Indian Ocean
4	Pacific Ocean
5	Ross Sea
6	Bellingshausen Amundsen Sea
11	Land
12	Coast

polemask.n08: A circular mask that symmetrically covers the observed maximum extent of the missing data (resulting from the orbit inclination and instrument swath) near the North Pole for DMSP-F8 and -F11. It consists of a standard 300-byte header, then a 2-dimensional byte array of 448 rows x 304 columns (332 x 316), stored in row order by columns. The circular mask is assigned the byte value of 1. Values outside the circle are assigned byte value of 0. Note that a similar mask for the Antarctic is neither supplied nor needed.

ltlnovrl.n (ltlnovr.s) - This is a 2-dimensional byte array containing latitude circles and longitude radials which can be superimposed on the Arctic (Antarctic) ice concentration images. The file consists of a standard 300-byte header, followed by a 2-dimensional byte array of 448 rows x 304 columns (332 x 316), stored by rows in column order. The circles and radials are assigned a byte value of 1 and the rest of the

grid, a value of 0.

Ocean Masks and images of maximum ice extent

Please see [Sea Ice Trends and Climatologies from SMMR and SSM/I](#) for details.

Related Data Collections

- [Sea Ice Products at NSIDC](#)

This site offers a complete summary of sea ice data derived from passive microwave sensors and other sources, and is useful for users who want to compare characteristics of various sea ice products to understand their similarities and differences. This site also provides links to tools for passive microwave data and a list of other sea ice resources.

- [Sea Ice Trends and Climatologies from SMMR and SSM/I](#)

NSIDC provides a suite of value-added products to aid in investigations of the variability and trends of sea ice cover. These products provide users with information about sea ice extent, total ice covered area, ice persistence, monthly climatologies of sea ice concentrations, and ocean masks.

- [Sea Ice Remote Sensing at NASA Goddard Space Flight Center](#)

4. Data Acquisition and Processing

Theory of Measurements

The SMMR and SSM/I instruments are microwave radiometers that sense emitted microwave radiation. This radiation is affected by surface and atmospheric conditions, and thus provides a range of geophysical information.

Source/Platform

The Nimbus and DMSP Block 5D-2 spacecraft fly in near polar sun-synchronous orbits.

Comparison of Orbital Parameters, SMMR, DMSP-F8, DMSP-F11 and DMSP-F13

Parameter	Nimbus-7 SMMR	DMSP-F8	DMSP-F11	DMSP-F13
Nominal Altitude*	955 km	860 km	830 km	850 km
Inclination Angle	99.1 degrees	98.8 degrees	98.8 degrees	98.8 degrees
Orbital Period	104 minutes	102 minutes	101 minutes	102 minutes

Ascending Node Equatorial Crossing (local time)	approximately 12:00 p.m.	approximately 6:00 a.m.	approximately 5:00 p.m.	approximately 5:43 p.m.
Algorithm Frequencies*	18.0, 37.0	19.4, 37.0	19.4, 37.0	19.4, 37.0
Earth Incidence Angle*	50.2	53.1	52.8	53.4
3 dB Beam Width (degrees)*	1.6, 0.8	1.9, 1.1	1.9, 1.1	1.9, 1.1

*Indicates sensor and spacecraft orbital characteristics of the three sensors used in generating the sea ice concentrations.

Source or Platform Objectives

SMMR

The Nimbus-7 SMMR was an experimental Earth-imaging passive microwave sensor launched as a follow-on to earlier experimental NASA radiometers (ESMR, NEMS, and SCAMS) launched by NASA on previous satellites in the Nimbus series (Nimbus-5 and -6). The SMMR was designed primarily for remote observations of oceanic, cryospheric, and tropospheric moisture-related phenomena. Key geophysical variables observable by the SMMR included sea surface temperature, sea surface wind speed, columnar water vapor over the ocean, cloud liquid water over the ocean, rain rate, sea ice concentration and type, snow extent and depth, and potentially other land parameters such as soil moisture, surface temperature, and vegetation extent.

SSM/I

The mission of the Defense Meteorological Satellite Program is to provide global coverage of visual and infrared cloud data and other specialized near real-time meteorological, oceanographic and solar-geophysical data required to support worldwide Department of Defense operations and high-priority programs. Timely data are supplied to Air Force Global Weather Central, the Navy Fleet Numerical Meteorology and Oceanography Center (FNMOC) and to deployed tactical receiving terminals worldwide.

The DMSP SSM/I advanced the SMMR instrumentation by improving resolution with the addition of an orthogonally polarized 85.5 GHz channel.

Sensor or Instrument Description

The SMMR is a ten-channel instrument delivering orthogonally polarized antenna temperature data at five dual-polarized (horizontal, vertical) frequencies, 6.6 GHz, 10.7 GHz, 18.0 GHz, 21.0 GHz, and 37.0 GHz. Please see the [SMMR Instrument Description](#) for more details.

The SSM/I is a seven-channel, four-frequency, orthogonally polarized, passive-microwave radiometric system. The instrument measures combined atmosphere and surface radiances at 19.3 GHz, 22.2 GHz, 37.0 GHz and 85.5 GHz. Please see the [SSM/I Instrument Description](#) for more details.

Data Acquisition Methods

The combined SMMR and SSM/I sea ice concentration time series is produced from brightness temperatures (T_B s) obtained from GSFC and NSIDC. The four sets of satellite data currently used to create this data stream and the periods for which the data are usable are: the Nimbus-7 SMMR from October 26, 1978 through August 20, 1987, the DMSP-F8 from July 9, 1987 through December 18, 1991, the DMSP-F11 from December 3, 1991 through December 31, 1996, and the DMSP-F13 from 5 May 1995 to present.

SMMR

Sea ice concentrations were processed by GSFC using SMMR T_B s. The SMMR T_B s were processed and quality checked at GSFC ([Gloersen et al. 1992](#)).

SSM/I

SSM/I F8, F11, and F13 data used to create the sea ice concentration time series are distributed by NSIDC. Processing of SSM/I F13 T_B s is ongoing. Data acquisition, filtering bad data, handling geolocation errors, implementation of an antenna pattern connection, and finally the swath-to-grid conversion are all described in the documentation for [DMSP SSM/I Daily and Monthly Polar Gridded Sea Ice Concentrations](#).

Derivation Techniques and Algorithms

(This section is extracted from [NASA Technical 104647](#))

Sea ice concentrations for this data set were derived from a revised NASA Team algorithm which uses a different set of tie points and weather filters than the original [NASA Team](#) algorithm.

Sea ice concentrations are produced from gridded T_B s using an algorithm employing three channels of the SMMR and four channels of the SSM/I instruments. The algorithm to obtain sea ice concentrations from SMMR uses the vertically and horizontally polarized T_B s at 18.0 GHz and vertically polarized brightness temperatures at 37.0 GHz ([Gloersen et al. 1992](#)). The NASA Team Algorithm ([Cavalieri et al. 1992](#)) uses the vertically and horizontally polarized T_B s at 19.4 GHz and the vertically polarized T_B s at 37.0 GHz to compute sea ice concentrations from the SSM/I F8 and F11 T_B s.

The weather filter used for the SMMR ([Gloersen and Cavalieri 1986](#)) was found to be inadequate for the SSM/I because of the latter's use of the 19.4 GHz channels (which are further up on the shoulder of the water vapor line at 22.2 GHz) rather than the 18.0 GHz channels. A different weather filter is used to reduce spurious sea ice concentrations from SSM/I that result from the presence of atmospheric water vapor, non-precipitating cloud liquid water, rain, and sea surface roughening by surface winds. This filter is a combination of the SSM/I 37.0 and 19.4 GHz channels, which effectively eliminates most of the spurious sea ice concentration measurements resulting from wind-roughening of the ocean surface, cloud liquid water, and rainfall. Another filter based on the 19.4 and 22.2 GHz channels is also used. The rationale behind combining the 19.4 and 22.2 GHz channels is based on the sensitivity of the 22.2 GHz to water vapor and on the need to minimize the effect of ice temperature variations at the ice edge.

Processing Steps

Comparisons of sea ice concentrations, calculated for each sensor during overlap periods using published

algorithm tie-points, reveal significant differences. These may result from differences in sensor and orbital characteristics, differences in observation times (and therefore tidal effects), or differences in algorithm coefficients. Sensor and orbital characteristic differences for the Nimbus-7 SMMR and DMSP-F8 SSM/I include antenna beam width, channel frequency, spacecraft altitude, ascending node time, and angle of incidence. In addition, the sea ice algorithm tie-points are significantly different. The F8, F11, and F13 sensors also differ in ascending node time, altitude, and angle of incidence. Because the visit times of the three satellites occur during different phases of the diurnal cycle, tidal effects may result in differences in the sea ice distribution. GSFC is presuming that any such effects are mitigated by the correction scheme described below. Comparison of orbital parameters for the SMMR, DMSP-F8, DMSP-F11, and DMSP-F13 in section 4 summarizes sensor and orbital characteristic differences. The GSFC processing attempts to accommodate for these differences in each pair of sensors by employing a self-consistent set of algorithm tie-points determined through linear relationships between the observed brightness temperatures during the overlap periods.

Nimbus-7 SMMR and DMSP-F8 SSM/I

Daily brightness temperature maps from the Nimbus-7 SMMR and from the DMSP-F8 SSM/I during their period of overlap, 9 July to 20 August 1987, were compared for both the Arctic and Antarctic. Unfortunately, there were only 22 days of common coverage. A linear, least squares best fit of the cumulative data was obtained for each of the corresponding channels. For the purpose of eliminating spurious brightness temperatures resulting from residual land spill over effects, an Arctic land mask expanded three to four pixels out from the original land mask was used in the determination of the best fit between the two data sets.

The eliminated pixels represent only a very small fraction of the total number of sea ice concentration pixels, but eliminating them helps considerably in reducing the outliers on the scatter plots. These linear relations were used to generate a set of SSM/I tie-points that are consistent with the original SMMR sea ice algorithm tie-points ([Gloersen et al. 1992](#)). The published SSM/I F8 tie-points ([Cavalieri et al. 1992](#)) were not used. In addition to using these transformations, the SSM/I F8 open water tie-points were subjectively tuned to help minimize the differences between the SMMR and SSM/I F8 sea ice extent and area during the overlap period. In all cases, except for the Antarctic F8 values, the tuned amount is within one standard error of estimate. GSFC suspects the reason for the larger tuned values results from greater weather effects during the overlap period.

For more information on the regression coefficients and revised tie points, refer to [NASA Technical Memorandum Number 104647](#).

DMSP-F8 and -F11 SSM/I

The period of overlap for F8 and F11 is even shorter than that for Nimbus-7 and SSM/I F8, with only 16 days of overlap of good data, from 3-18 December 1991. The SSM/I F11 open water tie-points were also tuned to help reduce differences in sea ice extent and area as was done with the SSM/I F8 values. A further adjustment to the Antarctic 37V sea ice type-B F11 tie-point was also made to reduce the sea ice area difference. In this case, the amount of tuning needed to reduce the sea ice extent and area differences between the F8 and F11 values is well within one standard error of estimate.

DMSP-F11 and -F13 SSM/I

The effects of changing from the SSM/I F11 to the F13 satellite are examined for a 5-month overlap period, from 5 May 1995 through 30 September 1995. Generally, in terms of hemispheric averages of mean ice concentration, the biases introduced by the switch from F11 to F13 are slight and are not statistically significant; however, in some regions relatively large and significant differences are seen. In addition, differences in sea ice extent and total ice-covered area between the two platforms were found to be statistically significant. For more information please see [NSIDC's Special Publication 5](#).

General Data Processing Steps

Land-to-Ocean Spill over and Residual Weather-Related Effects

The next step in preparing the data sets was the correction for land-to-ocean spill over (often referred to as "land contamination") and residual weather-related effects. Land-to-ocean spill over refers to the problem of blurring sharp contrasts in brightness temperature, such as exist between land and ocean, by the relatively coarse width of the sensor antenna pattern. This problem is of concern here because it results in false sea ice signals along coastlines. (Both land and sea ice have much higher brightness temperatures than ocean.) The method used to reduce the spill over is an extension of the method employed for the single-channel Nimbus-5 Electrically Scanning Microwave Radiometer (ESMR) data in [Parkinson et al. \(1987\)](#). The rationale behind the approach is that a minimum observed (generally in late summer) sea ice concentration in the vicinity of coastlines where no sea ice remains offshore is probably the result of land spill over and is thus subtracted from the image. To reduce the error of subtracting sea ice in areas of sea ice cover, the technique searches for and requires the presence of open water in the vicinity of the image pixel to be corrected.

Land-to-ocean spill over was reduced by the following three-step procedure:

- (1) A matrix M was created covering the entire grid and identifying each pixel as land, shore, near-shore, offshore, or non-coastal ocean. The identification of land pixels was straightforward, obtained from the land/sea mask. The identification of shore, near-shore, and off-shore pixels was based on the scheme plotted in Figure 1b, where the pixel to be identified is labeled I,J. This pixel is considered a "shore" pixel if any pixel adjacent to it is land, a "near-shore" pixel if none of the A pixels is land but at least one of the B pixels is land, and an "off-shore" pixel if none of the A or B pixels is land but at least one of the C pixels is land. All other ocean pixels are considered "non-coastal ocean". This matrix M is created once and then used throughout the data set.
- (2) A matrix CMIN, to represent minimum sea ice concentrations on a pixel-by-pixel basis throughout the entire grid, was created for each instrument type. CMIN was created by first constructing a matrix P containing the minimum monthly average sea ice concentrations throughout a given year, then adjusting that matrix at off-shore, near-shore, and shore pixels. In the case of SMMR, 1984 monthly data were used, whereas in the case of SSM/I, 1992 monthly data were used. In both cases, the adjustments were as follows: (a) at off-shore pixels, any P values exceeding 20% were reduced to 20%; (b) at near-shore pixels, any P values exceeding 40% were reduced to 40%; and (c) at shore pixels, any P values exceeding 60% were reduced to 60%. The CMIN matrix was created once for SMMR and once for SSM/I, then used throughout the data sets.
- (3) The daily sea ice concentration matrices for all three data sets were adjusted at any off-shore, near-shore, and shore pixels in the vicinity of open water. Specifically, the "neighborhood" of an off-shore pixel was defined as containing the 8 other pixels in the 3 x 3 box centered on the off-shore pixel; the "neighborhood" of a near-shore pixel was defined as containing the 24 other pixels in the 5 x 5 box centered on the near-shore pixel; and the "neighborhood" of a shore pixel was defined as containing the 48 other pixels in the 7 x 7 box centered on the shore pixel. At any time when the neighborhood of an off-shore, near-shore, or shore pixel contains three or more open-water pixels (i.e., sea ice concentration less than 15%), then the calculated sea ice concentration at the off-shore, near-shore, or shore pixel is reduced by the value for that pixel in the matrix CMIN. Wherever the subtraction leads to negative sea ice concentrations, the concentrations are set to 0%. This land-spillover -correction algorithm is clearly a rough approximation, as the contaminated amount does not stay constant over time; but the scheme has been found to reduce substantially the spurious sea ice concentrations on the grids.

An alternative method for reducing the effects of land contamination on summaries of the data is to use an

expanded land mask to limit the area under analysis ([Maslanik et al. 1996](#)).

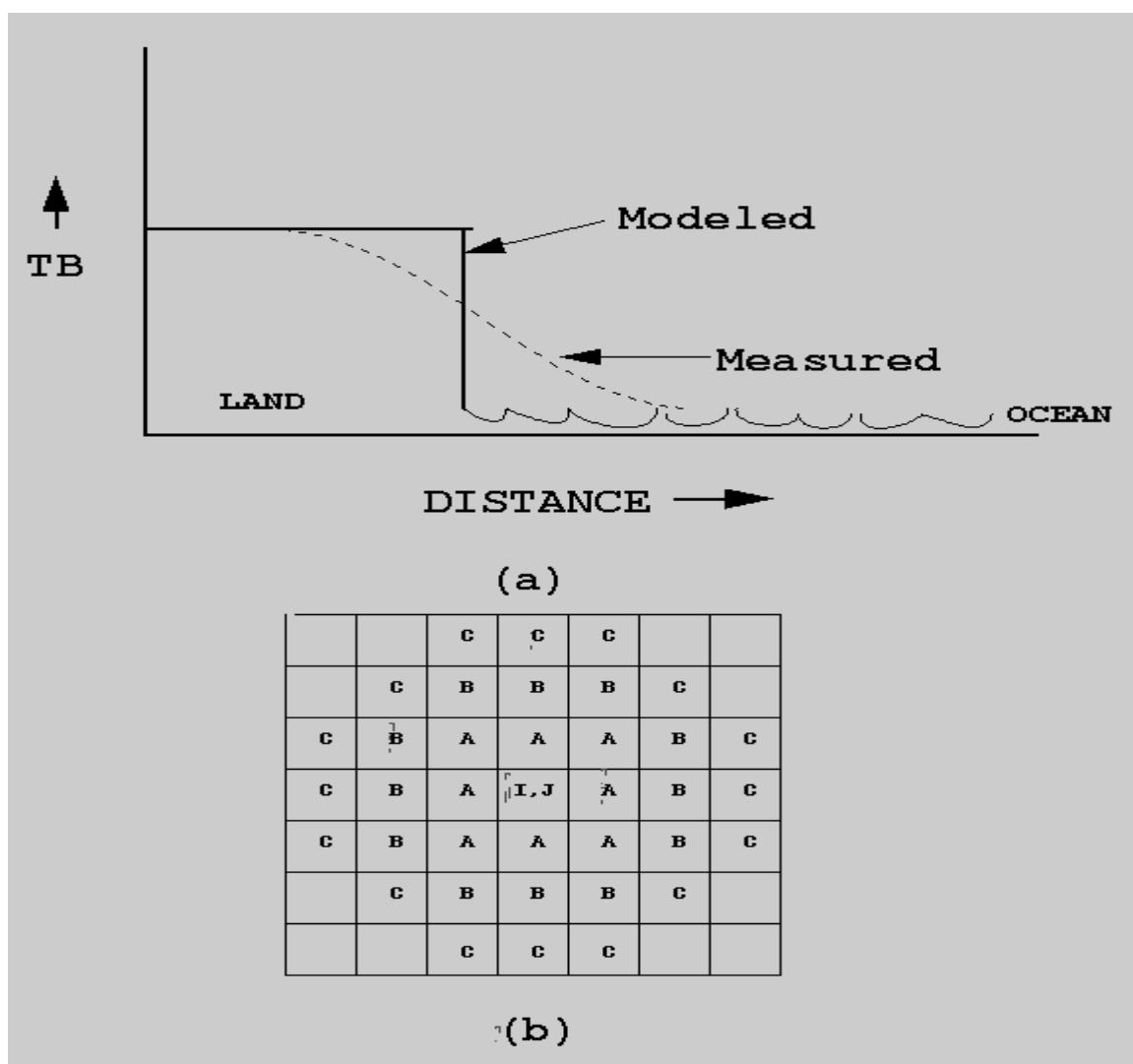
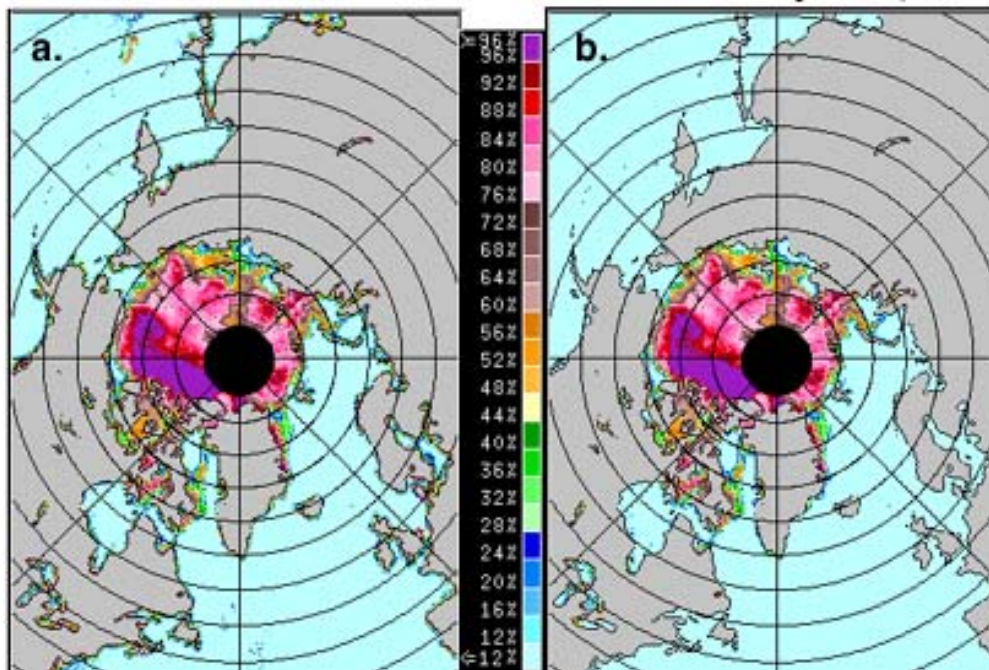


Figure a. Schematic illustrating the effect of the coarse resolution of the microwave antenna on a coastline. This effect, referred to as land-to-ocean spill over, results in false sea ice signals in the vicinity of the coast.
Figure b. Seven-by-seven array used in the procedure to reduce the land-to-ocean spill over effect.

Arctic SMMR Total Ice Concentration NIMBUS-7 Day 213 08/01/83



Sea ice concentration map of the Arctic for Day 213, 1983 **(a)** before and **(b)** after the application of the land spill over and residual weather corrections.

A correction for residual weather effects was made based on monthly climatological sea surface temperatures (SSTs) from the NOAA Ocean Atlas ([Levitus and Boyer 1994](#)). These data, originally on a 2 degree by 2 degree grid, were remapped onto the SSM/I grid. Because the SST data did not extend to the SSM/I coastline, the data were extrapolated to the coastline once regridded onto the SSM/I grid. The SST maps were used as follows:

In the Northern Hemisphere, in any pixel where the monthly SST is greater than 278 K, the sea ice concentration is set to zero throughout the month; in the Southern Hemisphere, wherever the monthly SST is greater than 275 K, the sea ice concentration is set to zero throughout the month. The higher threshold SST value was needed in the Northern Hemisphere because the 275 K isotherm used in the South was too close to the sea ice edge in the North. In a few instances, corrections to the regridded SST data were needed, because otherwise actual sea ice was being lost.

Note that while these steps eliminate much of the land-ocean spill over and weather effects over open ocean, these problems are not entirely removed. See the paragraph on [Data Verification](#) by Data Center in the following section for additional comments.

Filling Data Gaps

In each of the data sets, there are instances of missing data. In some cases whole days (or weeks or months) are missing. In other cases, large swaths or wedges of missing data exist within an image, along with scattered pixels of missing data throughout the grid. The scattered pixels of missing data, resulting generally from mapping the orbital data to the SSM/I grid, were filled by applying a spatial linear interpolation scheme on the brightness temperature maps. The larger areas of missing data, resulting from gaps between orbital swaths (generally at low latitudes on daily maps) or from partial coverage or missing days, were filled by temporal interpolation on the sea ice concentration maps. No data at all were available for the period from 2 December 1987 through 12 January 1988. This gap was not filled by temporal linear interpolation, instead being left as missing data.

Processing of Monthly Data

Nimbus-7 SMMR and DMSP SSM/I monthly averaged sea ice concentration grids were produced from an average of the daily sea ice concentration grids available for each month. Monthly files for both hemispheres are provided for every month beginning October 1978 and ending December 2004. Note however, that for October 1978, December 1987 and January 1988, the time series was incomplete and hence the monthly means for these months do not represent the "true" monthly means. For example, during October 1978, only three days were available to generate the monthly mean, only two days were available in December 1987, and for January 1988, the monthly mean is based on 19 days of daily data.

In most cases GSFC used all daily data to compute monthly averaged sea ice concentrations from a particular instrument until the data were no longer available. SMMR data, for example, were used to compute monthly sea ice concentrations until the instrument stopped collecting data on 20 August 1987. Beginning 21 August 1987, SSM/I F8 data were used. The file extensions for the monthly sea ice concentrations indicate which instrument was used. For example, August 1987 monthly sea ice concentrations are located in the 198708.N07 file. In September 1987, monthly sea ice concentrations are located in the 198706.N08 file. The *.N07 extension signifies that the monthly sea ice concentrations were derived using the NIMBUS-7 SMMR instrument, while '*.N08' identifies that the DMSP-F8 SSM/I instrument was used.

Data Notes

Since the goal of this data set is to provide a long term, consistent sea ice concentration product, it is necessary to address differences between the SMMR and the SSM/I F8, F11, and F13 sensors. Some problems were encountered when working with T_{BS} from sensors having different frequencies, different footprint sizes, different visit times, and different calibrations. A major obstacle to resolving these differences is the lack of sufficient overlapping data from sequential sensors. The techniques employed to solve these problems, or at least reduce their impacts, include: mapping the sensor data onto a common grid; applying a new land mask; addressing instrument drift; adjusting for land-ocean spill over; replacement of bad data; and inter-sensor corrections made to reduce remaining measurement differences. These techniques are discussed in more detail in the Derivation Techniques section of this document.

Note of Caution:

Computations of sea ice extents and sea ice areas should not be calculated from monthly-averaged ice concentration maps because using the monthly-averaged ice maps may result in a biased time series. It is recommended that sea ice extent and area be computed from daily maps of ice concentrations that are then used to compute monthly averages of those parameters. Documentation of the differences in sea ice extent and area between the daily concentrations and monthly-averaged concentrations is currently in progress. Upon completion, the web version of the documentation will be updated and users will be notified.

It is also important to know that SMMR and SSM/I have different data gaps at the North Pole due to orbital differences. Therefore, any time series of parameters, such as ice extent and ice covered area, need to take these differences into account. Polemasks for SMMR and SSM/I are provided in the OVLAY directory for this purpose. More information on these notes of caution is found on the [data help page](#).

5. References and Related Publications

See the following for background information pertaining to the instruments and sensor-level products used to generate the sea ice concentration time series. Other references, particularly for sea ice characteristics and

algorithm performance, are available in journals from the NSIDC library.

See also: [Selected Bibliography: SSM/I Brightness Temperatures for the Polar Regions](#).

Background on the Sea Ice Concentrations from Nimbus-7 SMMR and DMSP SSM/I Passive Microwave data set:

Cavalieri et al. (1997)

Background on the SMMR and SSM/I Sensors:

NSIDC Brightness Temperature User's Guide (1992), Gloersen and Barath (1977), Gloersen et al. (1992), Hollinger (1989), Hollinger and Lo (1983), Hollinger et al. (1990), Poe and Conway (1990), Svendsen et al. (1983), and Wentz (1991, 1992, 1993).

Raw sensor data and brightness temperatures:

See references above, Abdalati et al. (1995), and Goodberlet (1990).

Sea ice physics and characteristics:

Ackley (1979), Ackley et al. (1980), Wadhams et al. (1987), Carsey (1982), Gloersen et al. (1992). Also see the algorithm references below.

Passive microwave algorithms for sea ice:

Gloersen and Cavalieri (1986), Cavalieri et al. (1992), Cavalieri et al. (1984), Cavalieri (1994), Comiso (1983), Comiso (1990), Comiso et al. (1992), Comiso et al. (1984), Emery et al. (1994), Gloersen and Cavalieri (1986), Gloersen et al. (1992), Grenfell and Comiso (1986), Hollinger et al. (1984), Maslanik (1992), Massom (1991), Steffen and Schweiger (1991), Steffen et al. (1992), Svendsen et al. (1983), Swift and Cavalieri (1985), and Swift et al. (1985).

Applications of passive microwave-derived sea ice data:

Campbell et al. (1974, 1975a, 1975b, 1976a, 1976b, 1978, 1980a, 1980b, 1981, 1984, 1987), Carsey (1982, 1985), Cavalieri et al. (1983, 1986, 1990, 1991), Cavalieri and Parkinson (1981, 1987), Cavalieri and Martin (1985), Cavalieri and Zwally (1985), Comiso (1986, 1991), Comiso et al. (1992), Comiso and Sullivan (1986), Comiso et al. (1991), Gloersen et al. (1973, 1974a, 1974b, 1975a, 1975b, 1978, 1984, 1989, 1992), Gloersen and Campbell (1988a, 1988b, 1991a, 1991b), Maslanik et al. (1996), Massom (1991), Zwally (1984), Zwally et al. (1976, 1983a, 1983b, 1985), Zwally and Gloersen (1977), and Zwally and Walsh (1987).

Other algorithm, format, and processing issues:

Martino et al. (1995), NCSA (1993), Poe and Conway (1990), and Snyder (1982).

Abdalati, W., K. Steffen, C. Otto, and K.C. Jezek. 1995. Comparison of Brightness Temperatures from SSM/I instruments on the DMSP-F8 and -F11 satellites for Antarctica and the Greenland Ice Sheet. *International Journal of Remote Sensing*. 16(7):1223-1229.

Ackley, S.F. 1979. Mass balance aspects of Weddell Sea pack ice. *Journal of Glaciology* 24(90):391-406.

Ackley, S.F., A.J. Gow, K.R. Buck, and K.M. Golden. 1980. Sea ice studies in the Weddell Sea aboard USCGC Polar Sea. *Antarctic Journal of U. S.* 15(5):84-86.

Bonbright, D.I. 1984. *PODS SSM/I Functional Requirements (Version 1.0)*. Jet Propulsion Laboratory

Document 715-63.

Bonbright, D.I., J.W. Brown, J.E. Hilland, I.T. Hsu, J.A. Johnson, T.L. Kotlarek, R.A. Lassanyi, C.L. Miller, C.S. Morris, and F.J. Salamone. 1987. *NASA ocean data system version 3.0*. User handbook. Jet Propulsion Laboratory. Document 715-66, 50 pp.

Campbell, W.J. 1973. NASA remote sensing of sea ice in AIDJEX. *Proceedings of the World Meteorological Organization Technical Conference*, Tokyo, Japan, WMO No. 350:55-66.

Campbell, W.J., P. Gloersen, and H.J. Zwally. 1994. Short- and long-term temporal behavior of polar sea-ice covers from satellite passive-microwave observations. *Geophysical Monograph 85*. Editors O.M. Johannessen, R.D. Muench, and J.E. Overland. American Geophysical Union, Washington, D.C.

Campbell, W.J., P. Gloersen, and H.J. Zwally. 1984. Aspects of Arctic sea ice observable by sequential passive-microwave observations from the Nimbus-5 satellite, in *Arctic Technology and Policy*, I. Dyer and C. Chrysostomidis, eds., Hemisphere Publishing, New York, 197-222.

Campbell, W.J., P. Gloersen, and R.O. Ramseier. 1975. Synoptic ice dynamics and atmospheric circulation during the Bering Sea Experiment. *Proceedings of the Final Symposium on the Results of the Joint Soviet-American Expedition*, K. Ya. Kondratyev, Yu. I. Rabinovich, and W. Nordberg, eds., Gidrometeoizdat, Leningrad, 196-218. (Republished as USSR/USA Bering Sea Experiment by A. A. Balkema, Rotterdam, 307 pp., 1982.)

Campbell, W.J., P. Gloersen, E.G. Josberger, O.M. Johannessen, P.S. Guest, N. Mognard, R. Shuchman, B. A. Burns, N. Lannelongue, and K.L. Davidson. 1987. Variations of mesoscale and large-scale sea ice morphology in the 1984 Marginal Ice Zone Experiment as observed by microwave remote sensing. *Journal of Geophysical Research* 92:6805-6824.

Campbell, W.J., P. Gloersen, W. Nordberg, and T.T. Wilheit. 1974. Dynamics and morphology of beaufort sea ice determined from satellite, aircraft, and drifting stations, in *Proc. of the Symp. on Approaches to Earth Survey Problems Through Use of Space Techniques*, Akademie-Verlag, Berlin, 311-327.

Campbell, W.J., P. Gloersen, R.O. Ramseier, and H.J. Zwally. 1980. Arctic sea ice variations from time-lapse microwave imagery. *Boundary-Layer Meteorology* 18:99-106.

Campbell, W.J., P. Gloersen, W.J. Webster, T.T. Wilheit, and R.O. Ramseier. 1976. Beaufort Sea ice zones as delineated by microwave imagery. *Journal of Geophysical Research* 81:1103-1110.

Campbell, W.J., R.O. Ramseier, H.J. Zwally, and P. Gloersen. 1981. Structure and variability of Bering and Okhotsk sea ice cover by satellite microwave imagery, in *Energy Resources of the Pacific*, M. T. Halbouty, ed., American Association of Petroleum Geologists, Tulsa, Oklahoma, 343-354.

Campbell, W.J., P. Gloersen, H.J. Zwally, R.O. Ramseier, and C. Elachi. 1980. Simultaneous passive and active microwave observations of near-shore Beaufort Sea ice. *Journal of Petroleum Technology* 21:1105-1112.

Campbell, W.J., R.O. Ramseier, W.F. Weeks, and P. Gloersen. 1976. An integrated approach to the remote sensing of floating ice. *Proceedings of the XXVI International Astronautical Congress*, Lisbon, Portugal, L. G.

Napolitano, ed. 445-487.

Campbell, W.J., J. Wayenberg, J.B. Ramseyer, R.O. Ramseier, M.R. Vant, R. Weaver, A. Redmond, L. Arsenault, P. Gloersen, H.J. Zwally, T.T. Wilheit, T.C. Chang, D. Hall, L. Gray, D.C. Meeks, M.L. Bryan, F.T. Barath, C. Elachi, F. Leberl, and T. Farr. 1978. Microwave remote sensing of sea ice in the AIDJEX main experiment. *Boundary-Layer Meteorology* 13:309-337.

Campbell, W.J., W.F. Weeks, R.O. Ramseier, and P. Gloersen. 1975. Geophysical studies of floating ice by remote sensing. *Journal of Glaciology* 15:305-328.

Carsey, F.D. 1985. Summer Arctic sea ice character from satellite microwave data. *Journal of Geophysical Research* 90(C3):5015-5034.

Carsey, F.D. 1982. Arctic sea ice distribution at end of summer 1973-1976 from satellite microwave data. *Journal of Geophysical Research* 87:5809-5835.

Cavalieri, D.J. 1994. A microwave technique for mapping thin sea ice. *Journal of Geophysical Research* 99 (C6):12,561-12,572.

Cavalieri, D.J., and P. Gloersen. 1984. Determination of sea ice parameters with the Nimbus-7 SMMR. *Journal of Geophysical Research* 89(D4):5355-5369.

Cavalieri, D.J., P. Gloersen, C.L. Parkinson, J.C. Comiso, and H.J. Zwally. 1997. Observed hemispheric asymmetry in global sea ice changes. *Science* 278(5340): 1104-1106.

Cavalieri, D.J. and S. Martin. 1994. The contribution of Alaskan, Siberian, and Canadian coastal polynyas to the cold halocline layer of the Arctic Ocean. *Journal of Geophysical Research* 99:18,343-18,362.

Cavalieri, D.J., and S. Martin. 1985. A passive-microwave study of polynyas along the Antarctic Wilkes Land coast, in *Oceanology of the Antarctic Continental Shelf*, S. S. Jacobs, ed., Antarctic Research Series, American Geophysical Union, Washington, D. C. vol. 43:227-252.

Cavalieri, D.J., C.L. Parkinson, P. Gloersen, J.C. Comiso, and H.J. Zwally. 1999. Deriving long-term time series of sea ice cover from satellite passive-microwave multisensor data sets. *Journal of Geophysical Research* 104(7): 15,803-15,814.

Cavalieri, D.J., and C. L. Parkinson. 1987. On the relationship between atmospheric circulation and the fluctuations in the sea ice extents of the Bering and Okhotsk Seas. *Journal of Geophysical Research* 92: 7141-7162.

Cavalieri, D.J., and C.L. Parkinson. 1981. Large-scale variations in observed Antarctic sea ice extent and associated atmospheric circulation. *Monthly Weather Review* 109(11):2323-2336.

Cavalieri, D.J., and H.J. Zwally. 1985. Satellite observations of sea ice. *Advanced Space Research* 5:247-255.

Cavalieri, D.J., B.A. Burns, and R.G. Onstott. 1990. Investigation of the effects of summer melt on the calculation of sea ice concentration using active and passive-microwave data. *Journal of Geophysical Research* 95:5359-5369.

Cavalieri, D.J., P. Gloersen, and W.J. Campbell. 1984a. Determination of sea ice parameters with the Nimbus-7 SMMR. *Journal of Geophysical Research* 89:5355-5369.

Cavalieri, D.J., P. Gloersen, and W.J. Campbell. 1984b. Determination of sea ice parameters with the NIMBUS-7 SMMR. *Journal of Geophysical Research* 89(D4):5355-5369.

Cavalieri, D.J., P. Gloersen, and T.T. Wilheit. 1986. Aircraft and satellite passive-microwave observations of the Bering Sea ice cover during MIZEX West. *IEEE Transactions on Geosciences and Remote Sensing* GE-24: 368-377.

Cavalieri, D.J., S. Martin, and P. Gloersen. 1983. Nimbus-7 SMMR observations of the Bering Sea ice cover during March 1979. *Journal of Geophysical Research* 88:2743-2754.

Cavalieri, D.J., K.M. St. Germain, and C.T. Swift. 1995. Reduction of weather effects in the calculation of sea ice concentration with the DMSP SSM/I. *Journal of Glaciology*. 41(139):455-464.

Cavalieri, D.J., J. Crawford, M. Drinkwater, W.J. Emery, D.T. Eppler, L.D. Farmer, M. Goodberlet, R. Jentz, A. Milman, C. Morris, R. Onstott, A. Schweiger, R. Shuchman, K. Steffen, C.T. Swift, C. Wackerman, and R.L. Weaver. 1992. *NASA sea ice validation program for the DMSP SSM/I: final report*. NASA Technical Memorandum 104559. National Aeronautics and Space Administration, Washington, D.C. 126 pages.

Cavalieri, D.J., J. Crawford, M.R. Drinkwater, D. Eppler, L.D. Farmer, R.R. Jentz and C.C. Wackerman. 1991. Aircraft active and passive microwave validation of sea ice concentration from the DMSP SSM/I. *Journal of Geophysical Research* 96(C12):21,989-22,009.

Cavalieri, D.J., C.L. Parkinson, P. Gloersen, and H.J. Zwally. 1997. *Arctic and Antarctic sea ice concentrations from multichannel passive-microwave satellite data sets: October 1978 to December 1996, User's Guide*. NASA Technical Memorandum 104647. 17 pages.

Comiso, J.C. 1991. Satellite remote sensing of the polar oceans. *Journal of Marine Systems* 2:295-434.

Comiso, J.C. 1990. Arctic multiyear ice classification and summer ice cover using passive microwave satellite data. *Journal of Geophysical Research* 95(C8):13411-13422.

Comiso, J.C. 1986. Characteristics of Arctic winter sea ice from satellite multispectral microwave observations. *Journal of Geophysical Research* 91(C1): 975-994.

Comiso, J.C. 1983. Sea ice effective microwave emissivities from satellite passive microwave and infrared observations. *Journal of Geophysical Research* 88(C12):7686-7704.

Comiso, J.C., and A.L. Gordon. 1987. Recurring polynyas over the Cosmonaut Sea and the Maud Rise. *Journal of Geophysical Research* 92:2819-2833.

Comiso, J.C., and C.W. Sullivan. 1986. Satellite microwave and in-situ observations of the Weddell Sea ice cover and its marginal ice zone. *Journal of Geophysical Research* 91(C8):9663-9681.

Comiso, J.C., and H.J. Zwally. 1989. *Polar microwave brightness temperatures from Nimbus-7 SMMR*, NASA

RP-1223, 82 pages.

Comiso, J.C., and H.J. Zwally. 1984. Concentration gradients and growth/decay characteristics of the seasonal sea ice cover. *Journal of Geophysical Research* 89:8081-8103.

Comiso, J.C., and H.J. Zwally. 1982. Antarctic sea ice concentrations inferred from Nimbus-5 ESMR and Landsat imagery. *Journal of Geophysical Research* 87:5836-5844.

Comiso, J.C., S.F. Ackley, and A.L. Gordon. 1984. Antarctic sea ice microwave signatures and their correlation with in-situ ice observations. *Journal of Geophysical Research* 89(C1):662-672.

Comiso, J.C., T.C. Grenfell, D. Bell, M. Lange, and S. Ackley. 1989. Passive microwave in-situ observations of Weddell Sea ice. *Journal of Geophysical Research* 88(C12):7686-7704.

Comiso, J.C., T.C. Grenfell, M. Lange, A. Lohanick, R. Moore, and P. Wadhams. 1992. Microwave remote sensing of the Southern Ocean Ice Cover. Chapt. 12 In: *Microwave remote sensing of sea ice*. Frank Carsey, editor. American Geophysical Union. Washington, D.C. 243-259.

Comiso, J.C., and K. Steffen. 2001. Studies of Antarctic sea ice concentrations from satellite data and their applications. *Journal of Geophysical Research* 106(12): 31,361-31,385.

Comiso, J.C., P. Wadhams, W. Krabill, R. Swift, J. Crawford, and W. Tucker. 1991. Top/bottom multisensor remote sensing of Arctic sea ice. *Journal of Geophysical Research* 96(C2):2693-2711.

Emery, W.J., C. Fowler, J.A. Maslanik. 1994. Arctic sea ice concentrations from SSM/I and AVHRR satellite data. *Journal of Geophysical Research* 99(C9):18,329-18,342.

Eppler, D.T., L.D. Farmer, A.W. Lohanick, M.A. Anderson, D.J. Cavalieri, J.C. Comiso, P. Gloersen, C. Garrity, T.C. Grenfell, M. Hallikainen, J.A. Maslanik, C. Matzler, R. A. Melloh, I. Rubenstein, C.T. Swift. 1992. Passive microwave signatures of sea ice. In *Microwave Remote Sensing of Sea Ice*, ed. F. Carsey, Geophysical Monograph 68 (AGU).

Gloersen, P. 1995. Modulation of hemispheric sea ice covers by ENSO events. *Nature* 373:503-508.

Gloersen, P. 1983. *Calibration of the Nimbus-7 SMMR: II Polarization mixing corrections*. NASA Technical Memorandum 84976.

Gloersen, P. and F.T. Barath. 1977. A scanning multichannel microwave radiometer for Nimbus G and Seasat A. *IEEE Journal of Oceanic Engineering* OE-2:172-178.

Gloersen, P., and W.J. Campbell. 1991a. Variations of extent, area, and open water of the polar sea ice covers: 1978-1987, *Proc. of the Int. Conf. on the Role of the Polar Regions in Global Change*, G. Weller, C. L. Wilson, and B. A. B. Severin, eds., Geophysical Institute, University of Fairbanks, Alaska. 778 pages.

Gloersen, P., and W.J. Campbell. 1991b. Recent variations in Arctic and Antarctic sea ice covers. *Nature* 352:33-36.

Gloersen, P., and W.J. Campbell. 1988a. Variations in the Arctic, Antarctic, and global sea ice covers during

1978-1987 as observed with the Nimbus-7 Scanning Multichannel Microwave Radiometer. *Journal of Geophysical Research* 93:10,666-10,674.

Gloersen, P. and W.J. Campbell. 1988b. Satellite and aircraft passive-microwave observations during the Marginal Ice Zone Experiment in 1984. *Journal of Geophysical Research* 93:6837-6846.

Gloersen P. and D.J. Cavalieri. 1986. Reduction of weather effects in the calculation of sea ice concentration from microwave radiances. *Journal of Geophysical Research* 91(C3):3913-3919.

Gloersen, P. and A. Mernicky. 1997. Oscillatory behavior in Antarctic sea ice concentrations. In *AGU Antarctic Research Series: Antarctic Sea Ice Physical Properties and Processes*. Editor M.O. Jeffries. In press.

Gloersen, P., E. Mollo-Christensen, and P. Hubanks. 1989. Observations of Arctic polar lows with the Nimbus-7 Scanning Multichannel Microwave Radiometer, in *Polar and Arctic Lows*, P. F. Twitchell, E. A. Rasmussen, and K. L. Davidson, eds., A. Deepak, Hampton, Virginia, 359-371.

Gloersen, P., C.L. Parkinson, D.J. Cavalieri, J.C. Comiso, and H.J. Zwally. 1999. Spatial distribution of trends and seasonality in the hemispheric sea ice covers: 1978-1996. *Journal of Geophysical Research* 104(9): 20,827-20,835.

Gloersen, P., J. Yu, and E. Mollo-Christensen. 1996. Oscillatory behavior in Arctic sea ice concentrations. *Journal of Geophysical Research* 101:6641-6650.

Gloersen, P., W.J. Campbell, D.J. Cavalieri, J.C. Comiso, C.L. Parkinson, and H.J. Zwally. 1993. Satellite passive microwave observations and analysis of Arctic and Antarctic sea ice, 1978-1987. *Annals of Glaciology* 17:149-154.

Gloersen P., W.J. Campbell, D.J. Cavalieri, J.C. Comiso, C. L. Parkinson, H.J. Zwally. 1992. *Arctic and Antarctic Sea ice, 1978-1987: Satellite Passive Microwave Observations and Analysis*. NASA Special Publication 511.

Gloersen, P., D.J. Cavalieri, A.T.C. Chang, T.T. Wilheit, W.J. Campbell, O.M. Johannessen, K.B. Katsaros, K. F. Kunzi, D.B. Ross, D. Staelin, E.P.L. Windsor, F.T. Barath, P. Gudmandsen, E. Langham, and R.O. Ramseier. 1984. A summary of results from the first Nimbus-7 SMMR observations. *Journal of Geophysical Research* 89:5335-5344.

Gloersen, P., T.C. Chang, T.T. Wilheit, and W.J. Campbell. 1974. Polar sea ice observations by means of microwave radiometry, in *Advanced Concepts and Techniques in the Study of Snow and Ice*, H. S. Santeford and J. L. Smith, eds., National Academy of Science 541-550.

Gloersen, P., W. Nordberg, T.J. Schmugge, T.T. Wilheit, and W.J. Campbell. 1973. Microwave signatures of first-year and multiyear sea ice. *Journal of Geophysical Research* 78:3564-3572.

Gloersen, P., R.O. Ramseier, W.J. Campbell, T.C. Chang, and T.T. Wilheit. 1975. Variations of ice morphology of selected mesoscale test areas during the Bering Sea Experiment, in *Proceedings of the Final Symposium on the Results of the Joint Soviet-American Expedition*, K. Ya. Kondratyev, Yu. I. Rabinovich, and W. Nordberg, eds., Gidrometeoizdat, Leningrad, 196-218. (Republished as USSR/USA Bering Sea Experiment by A. A. Balkema, Rotterdam, 307 pages. 1982.)

Gloersen, P., R. Ramseier, W.J. Campbell, P.M. Kuhn, and W.J. Webster, Jr. 1975. Ice thickness distribution as inferred from infrared and microwave remote sensing during the Bering Sea Experiment, in *Proceedings of the Final Symposium on the Results of the Joint Soviet-American Expedition*, K. Ya. Kondratyev, Yu. I. Rabinovich, and W. Nordberg, eds., Gidrometeoizdat, Leningrad, 282-293. (Republished as USSR/USA Bering Sea Experiment by A. A. Balkema, Rotterdam, 307 pages. 1982.)

Gloersen, P., T.T. Wilheit, T.C. Chang, W. Nordberg, and W.J. Campbell. 1974. Microwave maps of the polar ice of the Earth. *Bulletin of the American Meteorological Society* 55:1442-1448.

Gloersen, P., H.J. Zwally, A.T.C. Chang, D.K. Hall, W.J. Campbell, and R.O. Ramseier. 1978. Time-dependence of sea ice concentration and multiyear ice fraction in the Arctic basin. *Boundary-Layer Meteorology* 13:339-359.

Goodberlet, M.A. 1990. *Special Sensor Microwave/Imager Calibration/Validation*. Ph.D. dissertation submitted to the University of Massachusetts.

Grenfell, T.C. and J.C. Comiso. 1986. Multifrequency passive microwave observations of first-year sea ice grown in a tank. *IEEE Transactions on Geoscience and Remote Sensing* GE-24:826-831.

Hollinger, J.P. 1989. *DMSP Special Sensor Microwave/Imager Calibration/Validation*. Naval Research Laboratory, Washington, D.C.

Hollinger, J.P. and R.C. Lo. 1983. *SSM/I Project Summary Report*. Naval Research Laboratory. NRL Memorandum Report 5055. 106 pages.

Hollinger, J.P., J.L. Pierce, and G.A. Poe. 1990. SSM/I instrument evaluation. *IEEE Transactions on Geoscience and Remote Sensing*, 28(5):781-790.

Hollinger, J.P., B.E. Troy, R.O. Ramseier, K.W. Asmus, M.F. Hartman, and C.A. Luther. 1984. Microwave emission from high Arctic sea ice during freeze-up. *Journal of Geophysical Research* 89(C5):8104-8122.

Hughes Aircraft Company. 1986. Data requirements document for Fleet Numerical Oceanography Center, Rev. B.

Hughes Aircraft Company. 1980. *Special Sensor Microwave Imager (SSM/I), computer program product specification (Specification for FNMOC)*. Vol. II, Sensor Data Processing, Computer Program Component (SMISDP).

Johannessen, O.M., W.J. Campbell, R. Shuchman, S. Sandven, P. Gloersen, E.G. Josberger, J.A. Johannessen, and P.M. Haugan. 1992. Microwave study programs of air-ice-ocean interactive processes in the seasonal ice zone of the Greenland and Barents Seas. In *Microwave Remote Sensing of Sea Ice*, ed. F. Carsey. Geophysical Monograph 68 (AGU).

Josberger, E.G., W.J. Campbell, P. Gloersen, A.T.C. Chang, and A. Rango. 1993. A hydrology of the upper Colorado River Basin derived from satellite passive-microwave observation. *Annals of Glaciology* 17:322-331.

Josberger, E.G., P. Gloersen, A.T.C. Chang, A. Rango. 1996. The effects of snowpack grain size on the

passive microwave signatures from the upper Colorado river basin snowpack. *Journal of Geophysical Research* 101:6679-6688.

Levitus, S. and Boyer, T.P. 1994. World Ocean Atlas 1994, Volume 4: Temperature, NOAA National Oceanographic Data Center, Ocean Climate Laboratory, U.S. Department of Commerce, Washington D.C.

Martino, M.G., D.J. Cavalieri and P. Gloersen. 1995. *An improved land mask for the SSM/I Grid*. NASA Technical Memorandum TM104625.

Maslanik, J.A. 1992. Effects of weather on the retrieval of sea ice concentration and ice type from passive microwave data. *International Journal of Remote Sensing* 13(1):37-54.

Maslanik, J.A., M.C. Serreze, and R.G. Barry. 1996. Recent decreases in Arctic summer sea ice cover and linkages to atmospheric circulation anomalies. *Geophysical Research Letters* 23(13):1677-1680.

Massom, R.A. 1991. *Satellite remote sensing of polar regions*. Boca Raton: Lewis Publishing.

National Center for Supercomputing Applications. 1993. *Getting started with HDF*. Draft Version 3.2. page 44.

Parkinson, C.L. 1995. Recent sea-ice advances in Baffin Bay/Davis Strait and retreats in the Bellingshausen Sea. *Annals of Glaciology* 21:348-352.

Parkinson, C.L. 1994. Spatial patterns of increases and decreases in the length of the sea ice season in the Southern Ocean, 1979-1986. *Journal of Geophysical Research* 99:16,327-16,339.

Parkinson, C.L. 1992a. Spatial patterns of increases and decreases in the length of the sea ice season in the North Polar region, 1979-1986. *Journal of Geophysical Research* 97:14,377-14,388.

Parkinson, C.L. 1992b. Interannual variability of monthly Southern Ocean sea ice distributions. *Journal of Geophysical Research* 97:5349-5363.

Parkinson, C.L. 1991. Interannual variability of the spatial distribution of sea ice in the north polar region. *Journal of Geophysical Research* 96:4791-4801.

Parkinson, C.L. 1990. The impact of the Siberian High and Aleutian Low on the sea ice cover of the Sea of Okhotsk. *Annals of Glaciology* 14:226-229.

Parkinson, C.L. 1983. On the development and cause of the Weddell Polynya in a sea ice simulation. *Journal of Physical Oceanography* 13:501-511.

Parkinson, C.L., and R.A. Bindshadler. 1984. Response of Antarctic sea ice to uniform atmospheric temperature increases, in *Climate Processes and Climate Sensitivity*, J. E. Hansen and T. Takahashi, eds., Maurice Ewing Series, Vol. 5, American Geophysical Union, Washington, D. C., pp. 254-264.

Parkinson, C. L., and D. J. Cavalieri. 2002. A 21-year record of arctic sea-ice extents and their regional, seasonal, and monthly variability and trends. *Annals of Glaciology* 34: 441-446.

Parkinson, C. L., D. J. Cavalieri, P. Gloersen, H. J. Zwally, and C. Comiso. 1999. Arctic sea ice extents, areas, and trends, 1978-1996. *Journal of Geophysical Research* 104(9): 20,837-20,856.

Parkinson, C.L., and D.J. Cavalieri. 1989. Arctic sea ice, 1973-1987: Seasonal, regional, and interannual variability. *Journal of Geophysical Research* 94:14,499-14,523.

Parkinson, C.L., and D.J. Cavalieri. 1982. Interannual sea ice variations and sea ice/atmosphere interactions in the Southern Ocean, 1973-1975. *Annals of Glaciology* 3:249-254.

Parkinson, C.L., and P. Gloersen. 1993. Global Sea Ice Coverage. In *Atlas of Satellite Observations Relate to Global Change*. Editors R. Gurney, J. Foster, and C. Parkinson. Cambridge University Press.

Parkinson, C.L., and A.J. Gratz. 1983. On the seasonal sea ice cover of the Sea of Okhotsk. *Journal of Geophysical Research* 88:2793-2802.

Parkinson, C.L., J.C. Comiso, H.J. Zwally, D.J. Cavalieri, P. Gloersen, and W.J. Campbell. 1987. *Arctic Sea Ice, 1973-1976: Satellite Passive-Microwave Observations*, NASA SP-489, National Aeronautics and Space Administration, Washington, D.C. 296 pages.

Pearson, F. 1990. Map projections: Theory and applications. CRC Press. Boca Raton, Florida. 372 pages.

Poe, G.A. and R.W. Conway. 1990. A study of the geolocation errors for the Special Sensor Microwave/Imager (SSM/I). *IEEE Transactions on Geoscience and Remote Sensing* 28(5):791-799.

Rothrock, D.A., D.R. Thomas, and A.S. Thorndike. 1988. Principal component analysis of satellite passive-microwave data over sea ice. *Journal of Geophysical Research* 93:2321-2332.

Shuchman, R.A., B. Burns, O.M. Johannessen, E.G. Josberger, W.J. Campbell, T. Manley, and N. Lannelongue. 1987. Remote sensing of the Fram Strait marginal ice zone. *Science* 236:429-431.

Shuchman, R.A., W.J. Campbell, B. Burns, E. Ellingsen, B. Farrelly, P. Gloersen, T. Grenfell, J. Hollinger, D. Horn, J. Johannessen, O. Johannessen, E. Josberger, C. Livingstone, C. Luther, T. Manley, R. Markson, C. Mätzler, E. Mollo-Christensen, R. Onstott, D. Ross, S. Sandven, C. Schgoun, A. Stiffey, E. Svendsen, G. Simmonds, and Z. Top. 1984. Remote sensing of the Marginal Ice Zone Experiment, in *Proceedings of the IGARSS'84 Symposium*, Strasbourg, France, European Space Agency, ESA SP-215, 404-409.

Snyder, J.P. 1987. Map projections - a working manual. U.S. Geological Survey Professional Paper 1395. U. S. Government Printing Office. Washington, D.C. 383 pages.

Snyder, J.P. 1982. *Map Projections Used by the U.S. Geological Survey*. U.S. Geological Survey Bulletin 1532.

Steffen, K. and A. Schwieger. 1991. NASA Team algorithm for sea ice concentration retrieval from Defense Meteorological Satellite Program Special Sensor Microwave/Imager: Comparison with Landsat satellite imagery. *Journal of Geophysical Research* 96(C12):21,971-21,988.

Steffen, K., D.J. Cavalieri, J.C. Comiso, K. St. Germain, P. Gloersen, J. Key, and I. Rubinstein. 1992. The estimation of geophysical parameters using passive microwave algorithms. Chapt 10 In *Microwave remote*

sensing of sea ice. Frank Carsey, editor. American Geophysical Union. Washington, D.C. 243-259.

Sullivan, C.W., C.R. McClain, J.C. Comiso, and W.O. Smith, Jr. 1988. Phytoplankton standing crops within an Antarctic ice edge assessed by satellite remote sensing. *Journal of Geophysical Research* 93:12,487-12,498.

Svendsen, E., K. Kloster, B. Farrelly, O. M. Johannessen, J. A. Johannessen, W.J. Campbell, P. Gloersen, D. Cavalieri, and C. Matzler. 1983. Norwegian Remote Sensing Experiment: Evaluation of the Nimbus-7 scanning multichannel microwave radiometer for sea ice research. *Journal of Geophysical Research* 88 (C5):2781-2791.

Swift, C.T. 1980. Passive-microwave remote sensing of ocean-A review. *Boundary-Layer Meteorology* 18:25-54.

Swift, C.T., D.J. Cavalieri. 1985. Passive microwave remote sensing for sea ice research. *EOS* 66(49):1210-1212.

Swift, C.T., Fedor, L.S. and Ramseier, R.O. 1985. An algorithm to measure sea ice concentration with microwave radiometers. *Journal of Geophysical Research* 90(C1):1087-1099.

Wadhams, P., M.A. Lange, and S.F. Ackley. 1987. The ice thickness distribution across the Atlantic sector of the Antarctic ocean in midwinter. *Journal of Geophysical Research* 92(C13):14,535-14, 552.

Walsh, J.E., and C.M. Johnson. 1979. Interannual atmospheric variability and associated fluctuations in Arctic sea ice extent. *Journal of Geophysical Research* 84:6915-6928.

Walsh, J.E., and H.J. Zwally. 1990. Multiyear sea ice in the Arctic: model- and satellite-derived. *Journal of Geophysical Research* 95:11,613-11,628.

Wentz, F.J. 1993. *User's manual: SSM/I antenna temperature tapes: rev. 2*. Remote Sensing Systems, Inc. Santa Rosa, CA. RSS Technical Report 120193.

Wentz, F.J. 1992. *Final report, production of SSM/I data sets*. Remote Sensing Systems, Inc., Santa Rosa, CA. RSS Technical Report 090192.

Wentz, F.J. 1991. *User's manual: SSM/I antenna temperature tapes*. Remote Sensing Systems, Inc., Santa Rosa, CA. RSS Technical Report 032588.

Zwally, H.J. 1984. Observing polar-ice variability. *Annals of Glaciology* 5:191-198.

Zwally, H.J., and P. Gloersen. 1993. Variability of the Arctic perennial ice pack. In *Proceedings of the International Symposium on ISY Polar Ice Extent, February 1993*. Editor F. Nishio. 127-132. National Space Development Agency, Mombetsu, Japan.

Zwally, H.J., and P. Gloersen. 1977. Passive-microwave images of the polar regions and research applications. *Polar Records* 18:431-450.

Zwally, H.J., and J.E. Walsh. 1987. Comparison of observed and modeled ice motion in the Arctic Ocean. *Annals of Glaciology* 9:136-144.

Zwally, H.J., J.C. Comiso, and A.L. Gordon. 1985. Antarctic offshore open water within the pack and oceanographic effects, in *Oceanology of the Antarctic Continental Shelf*, S. S. Jacobs, ed., Antarctic Research Series vol. 43, American Geophysical Union, Washington, D. C. 203-226.

Zwally, H.J., C.L. Parkinson, and J.C. Comiso. 1983. Variability of Antarctic sea ice and changes in carbon dioxide. *Science* 220:1005-1012.

Zwally, H.J., J.C. Comiso, C.L. Parkinson, W.J. Campbell, F.D. Carsey, and P. Gloersen. 1983. *Antarctic Sea Ice, 1973-1976: Satellite Passive-Microwave Observations*, NASA SP-459, National Aeronautics and Space Administration, Washington, D.C. 206 pages.

Zwally, H.J., T.T. Wilheit, P. Gloersen, and J.L. Mueller. 1976. Characteristics of Antarctic sea ice as determined by satellite-borne microwave imagers, in *Proceedings of the Symposium on Meteorological Observations from Space: Their Contribution to the First GARP Global Experiment*, Committee on Space Research of the International Council of Scientific Unions, Philadelphia, 94-97.

6. Document Information

Glossary and Acronyms

Please see the [EOSDIS Glossary of Terms](#) for a general list of terms.

List of Acronyms

Please see the [EOSDIS Acronyms](#) list for a general list of Acronyms. The following acronyms are used in this document:

ANSI: American National Standards Institute

ASCII: American Standard Code for Information Interchange

CIRES: Cooperative Institute for Research in Environmental Sciences

DMSP: Defense Meteorological Satellite Program

DOS: Disk Operating System

ESMR: Electrically Scanning Microwave Radiometer

FNMO: Fleet Numerical Meteorology and Oceanography Center

FTP: File Transfer Protocol

GIF: Graphical Interchange Format

GSFC: Goddard Space Flight Center

IDL: Interactive Data Language

NASA: National Aeronautics and Space Administration

NEMS: Nimbus-E Microwave Spectrometer

NOAA: National Oceanic and Atmospheric Administration

NSIDC: National Snow and Ice Data Center

PNG: Portable Network Graphics

SCAMS: Scanning Microwave Spectrometer

SSM/I: Special Sensor Microwave/Imager

SMMR: Scanning Multichannel Microwave Radiometer

SST: Sea Surface Temperature

T_B: Brightness temperature

Document Creation Date

1996

Document Revision Date

February 2006

Document URL

http://nsidc.org/data/docs/daac/nsidc0051_gsfc_seaice.gd.html